2020 International Symposium on Nonlinear Theory and Its Applications,
NOLTA2020, Virtual, November 16-19, 2020

Multiple control of two-dimensional optical bistable device for encoding of complex maze

Takashi ISOSHIMA

Nano Medical Engineering Laboratory, Cluster for Pioneering Research (CPR), RIKEN
2-1 Hirosawa, Wako, Saitama 351-0198, Japan
Email: isoshima@riken.jp

Abstract– Bistable system with a spatial expanse can present a traveling wavefront, an interface between two stable states. We investigate a two-dimensional optical bistable device (2DOBD) for natural computing including maze exploration. We have reported that our device can present both extension and reduction of “on”-state area controlled not only by the light intensity but also the path width, a geometrical parameter. In this paper we consider possibility of encoding a “complex” maze with another feature such as conductance or altitude in addition to the topological connectivity, utilizing our multi-parameter controllability in 2DOBD.

1. Introduction

In a bistable system with a spatial expanse, the two stable states can coexist occupying different areas in the system. The interface between the areas of two stable states - in this paper we call them "on" and "off" states - travels like a wavefront [1]. We are investigating such wavefront propagation in a two-dimensional bistable device for information processing, as a kind of natural computing. Natural computing is an information processing scheme utilizing dynamics of various natural phenomena, and attracting attentions as an alternative to the digital computing on the silicon-based integrated circuits. Exploration of a maze is a popular application of natural computing, and various natural phenomena have been tried to solve a maze: chemical reaction wave in an excitable Belousov-Zhabotinsky (BZ) medium [2], a self-propelling oil droplet in aqueous solution of amphiphilic reagent with pH gradation [3], extension and shrinkage of a true slime mold [4], and so on.

Here we employ a two-dimensional thermo-optical bistable device (2DOBD) as the medium for wavefront propagation to explore a maze. In previous works [5-9], we have revealed that the wavefront of "on"-state area in a 2DOBD presents extension and reduction (retreat) behavior controlled by the irradiated light intensity, that Steinbock maze can be explored, and that the wavefront velocity is also controllable geometrically. In this work, we investigate more detailed property of wavefront velocity control by the path width, and present demonstration of the effect of width control in Steinbock maze exploration.

2. Two-dimensional optical bistable device (2DOBD)

Bistability can be realized by a positive feedback and nonlinearity. Pure optical bistability is realized using, for example, a Fabry-Perot resonator filled with an optical Kerr medium: the resonator provides feedback and the medium provides nonlinearity. This device works very fast, but requires large optical intensity for operation, usually provided by a femtosecond pulse laser. Another type of optical bistability is thermo-optical bistability, realized by interaction between temperature, temperature-dependent optical property change (usually this contains nonlinearity), and heat generated by light.

We have designed a device composed of a liquid crystal and an optical absorber. The liquid crystal shows phase transition between isotropic and nematic phases at a certain temperature. For example, 4-Cyano-4'-pentylbiphenyl (5CB) shows the phase transition at about T_{PT} = 35 °C. Below T_{PT}, 5CB is in the nematic phase and looks opaque, thus the optical transmission is low due to light scattering. Above T_{PT}, 5CB is transparent in the isotropic phase. Thus 5CB presents nonlinear behavior in the optical transmission as a function of temperature. The device is composed of a top cover, the 5CB layer, and a black bottom substrate. The substrate absorbs light transmitted through the 5CB layer, generating heat from light. Assuming that the temperature of the whole device is below T_{PT}, 5CB is in nematic phase and opaque. Light from the top side is scattered in 5CB layer and only small fraction of the light is absorbed by the bottom black layer. Increasing the intensity of light, the heat by photoabsorption also increases. Finally the local temperature reaches T_{PT} and 5CB starts phase transition to isotropic phase, becoming transparent. This further increases heat generation and thus temperature, functioning as the positive feedback to cause transition to the high transmission "on" state. Once turned on, even if the light intensity decreases, the device stays in "on" state until the light becomes significantly weaker than the turn-on threshold, presenting the hysteresis property in the light intensity vs. transmission curve. In this hysteresis region of light intensity, the device presents bistability.

With a spatial expanse, the device can provide wavefront propagation. Under irradiation of bias light at the bistable intensity, the whole area of the device can stay at the ‘'off" (low transmission) state at the beginning. If sufficiently strong light is irradiated to a small area on the device, it is *locally* triggered to the "on" state. The turn-on wavefront can expand two-dimensionally due to thermal

diffusion. In maze exploration, a maze pattern is irradiated on the device, the path area irradiated with a higher intensity light and the wall area with a lower intensity light. Exploration starts by irradiating strong trigger light at the start point of the maze.

3. Numerical Simulation Method

The dynamic behavior of a thermo-optical 2DOBD can be modeled using a thermal diffusion equation containing heat generation by photoabsorption, as follows: [5-9]

$$\frac{\partial T}{\partial t} = \Delta T + \sigma - \rho \quad (1)$$

$$\sigma = A(T)\, I \quad (2)$$

$$\rho = \alpha\, T \quad (3)$$

Here t stands for the time, T the temperature as a function of spatial coordinates and time, σ the generated heat, ρ the heat dissipation at the surface to outside of the device, A the temperature-dependent optical absorption, I the incident light intensity, and α the heat dissipation coefficient (heat resistance) [6-9]. Nonlinearity essential for the bistability is included in the term $A(T)$.

Time-dependent three-dimensional (3-D) numerical simulation was performed by means of the finite element method using FreeFEM++ Ver.3.41 software [10]. The device structure used in the numerical simulation is shown in Fig.1. Using this device structure, we are also trying experimental demonstration, which will be reported separately in future. The materials assumed here are same as our experimental device. Acrylic polymer is used for the the top cover and bottom substrate. Bottom surface of the substrate is contacted to a temperature-controlled hot plate kept at 30 °C. The top cover and side wall of the device is exposed to air at 25 °C. Thicknesses of the top cover, 5CB layer, black layer, and bottom substrate were 0.2, 0.1, 0.02, and 1.0 mm, respectively. Optical absorption of the black layer is 100 %. Thermal diffusion constant of acrylic polymer and 5CB is 0.92 and 1.0 [10^{-3} cm^2 s^{-1}], respectively. Heat dissipation constant (heat resistance) at the boundary of the device is 0.92×10^{-2} [W $°C^{-1}$]. In the simulation of wavetfront propagation to investigate dependency on the path width, adaptive mesh method starting from 0.5 mm element size was employed

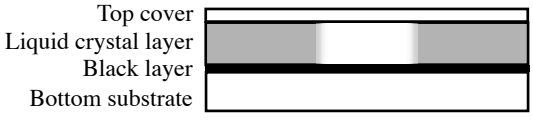

Figure 1: Schematic cross-section of the thermo-optical bistable device based on nematic-isotropic phase transition of a liquid crystal 5CB. The top cover and the bottom substrate compose a cell structure encapsulating the liquid crystal 5CB. The light irradiated from the top side transmits through the 5CB layer and is absorbed in the black layer to generate heat. 5CB presents lower optical transmission due to optical scattering at a temperature lower than 35°C (in nematic phase, shown in grey), while it shows higher transmission at a temperature higher than 35°C (in isotropic phase, shown in white). The wavefront (interface between the grey and white area) can propagate laterally.

to follow the path width change by 0.2 mm. This costed mild increase of calculation time, while providing much higher precision in the simulated results. Time step for sequentially solving the differential equation was 2 sec. In the simulation of Steinbock maze exploration, fixed element size of 0.5mm and time step of 30 sec was employed. Temperature-dependent transmission of 5CB layer is approximated to be 0.5 at 35 °C or lower, 1.0 at 37 °C or higher, and linearly increasing from 0.5 to 1.0 in the temperature range of 35 to 37 °C. Light intensity was 0.250 and 0.154 W/cm² at the path and the wall area of the maze, respectively, if not described explicitly. Trigger light intensity was 0.450 W/cm². For investigating the dependence on the path width, specially designed test maze pattern was employed [7-9], which was much smaller and simpler than Steinbock maze. The test path was kept as wall area (irradiated by weak light of 0.154 W/cm²) for the first 200 sec, and then the light intensity increased to the specified value for the path, so that the on area extends through the finger. The wavefront position varies as a function of time, and thus the wavefront velocity can be obtained as the slope by fitting to a linear function. Various widths of the finger pattern W ranging from 0.8 to 2.8 mm were used in the numerical simulation.

3. Results and Discussions

We have already presented in a previous paper that the wavefront velocity can be controlled by the path width [9]. Here we investigate the dependence of wavefront velocity on the two parameters, path width and light intensity at the path. Figure 2 shows wavefront velocity as functions of path width, at a range of light intensity at the path from 0.214 to 0.250 W/cm². Positive velocity stands for the extension mode, and negative one for the reduction mode. Wavefront velocity increases with the path width and the light intensity at the path. Sudden drops of the velocity below -5×10^{-3} cm/s correspond to the lower threshold in the hysteresis curve of the bistable system at

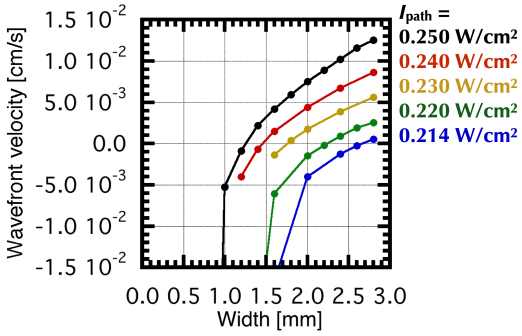

Figure 2: Dependence of wavefront velocity on the path line width and light intensity on the path I_{path}. Each line shows the velocity-width relation at the light intensity on the path of 0.250, 0.240, 0.230, 0.220, and 0.214 W/cm² (from to p to bottom), respectively. The light intensity at the wall area was fixed to 0.154 W/cm². In some cases, significant decrease of the velocity was obtained at narrower width, which was out of the range of the graph and just the lines were plotted.

a static condition, meaning that the "on" state cannot be held even in the connected path area. The velocity dependence on the path width is sub-linear, showing saturating behavior at wider path. This is elucidated by the balance of heat and effect of the border around the "on" area. Not only at the "front" border but also at the side borders, the heat generated in the "on" area by photoabsorption dissipates. If the path is wider, the influence of the side borders becomes relatively small, and eventually in the case of infinite width only the front border affects and the velocity reaches to a finite maximum value.

Figure 3 shows an operational mode mapping, or a "phase diagram" on the plane of the path width and light intensity at the path. The red points show the extension mode, and the blue ones the reduction mode. The border between the extension and reduction modes runs from top-left to bottom-right, presenting a compensating relation between the light intensity and path width.

Such flexibility in controllable parameters can be applied to modified maze exploration. In a maze having a three-dimensional (3D) terrain, altitude or slope of the path can be encoded by modifying the width: narrower width for an ascending slope presents lower velocity of wavefront propagation. In a traffic analysis of a highway network, the width of the road (or the number of lanes) can be encoded to the path width, resulting in faster propagation in a wider path. These can be combined to

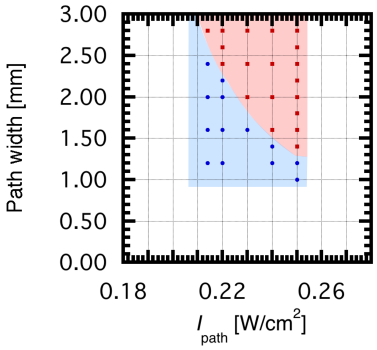

Figure 3: Phase diagram, or operational mode mapping on the plane of the light intensity and width of the path area in 2DOBD. The light intensity at the wall area was fixed to 0.154 W/cm^2. Red dots show the conditions for the extension mode, and blue ones for the reduction mode. Red and blue background colors are for guiding eyes, and the border was not obtained rigorously.

simulate a highway network with a 3D terrain: path width encodes for the number of lanes, and light intensity at a path for the slope. Although the encoding functions must be designed carefully, multiple controllable parameters in 2DOBD will enable us flexible application.

Figure 4 shows exploration of a maze with modified path width. Steinbock maze pattern presents double paths, and one pair exists at top-left corner. In this simulation, the path marked in red in Fig.4(a) was narrowed from 3.0

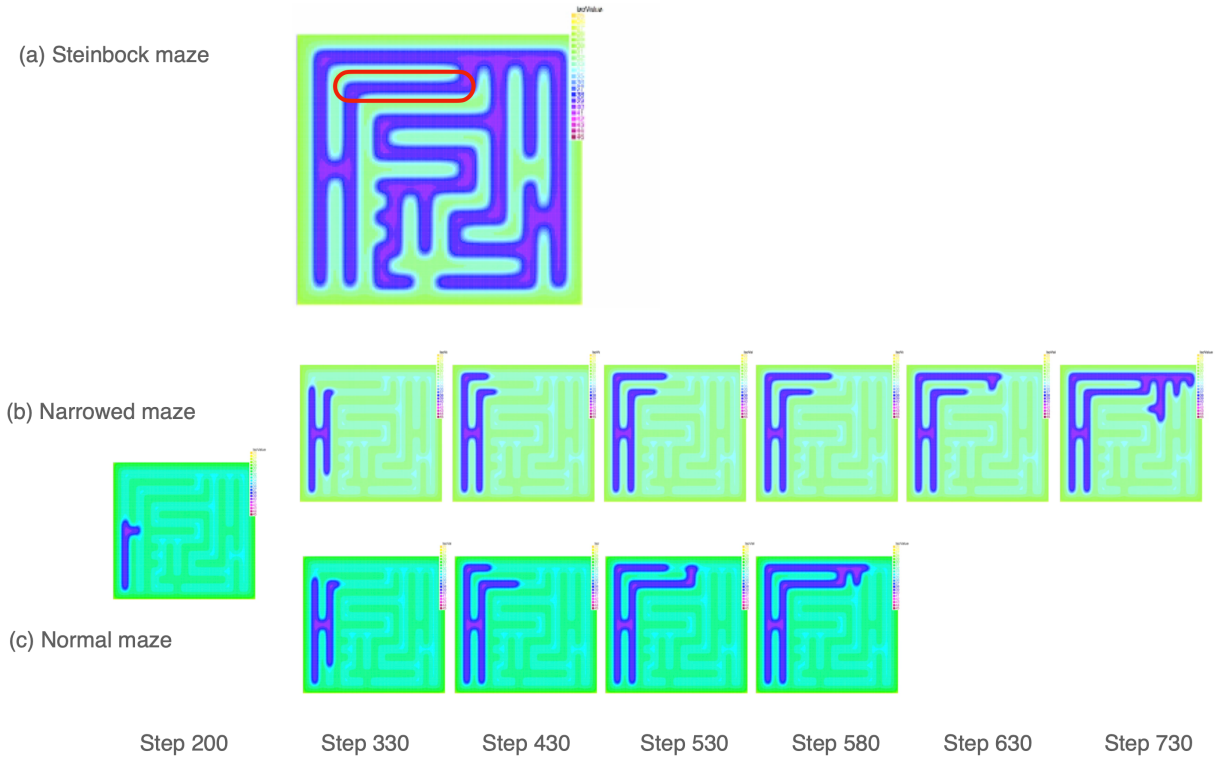

Figure 4: Modulation of wavefront propagation velocity in Steinbock maze exploration. (a) Steinbock maze pattern was shown in blue. The path surrounded by red line was narrowed from 3.0 mm to 2.5 mm width. (b) Temporal evolution of the "on" area (shown in blue) in the narrowed maze. 1 step corresponds to 30 sec. (c) Temporal evolution of the "on" area in the normal (unmodified) maze. At step 200, the "on" area goes into the blanches, and the "on" area in the bottom blanch reaches to the joining point at step 530 in the normal maze. In the narrowed maze, the extension of "on" area in the bottom branch is slower and the "on" area in the top blanch reaches to the joining point earlier (at step 630). Finally the "on" areas in both blanch merges at step 730 for the narrowed maze and step 580 for the normal maze.

to 2.5 mm. Temporal evolution of the extension of "on" area for the (b) maze with the narrowed path and (c) unmodified Steinbock maze with a constant path width of 3.0 mm was compared. As expected, extension velocity in the narrowed path was significantly slower, and the order of reaching at the joining point from the two paths changed. The narrow path can be interpreted as a narrow or up-climbing road resulting in slower traffic.

These results demonstrate that the wavefront propagation in the 2DOBD is controllable by a geometrical parameter, the width of the maze path, in addition to the light intensity.

4. Concluding Remarks

In this paper, we have reported the operation of 2DOBD by the numerical simulation using finite element method, and presented that the wavefront velocity can be controlled by two parameters, the path width of the maze and the light intensity at the path. Phase diagram presented some compensating relation between the two parameters. Having two controllable parameters will provide additional flexibility to the natural computing based on 2DOBD. Encoding the altitude and road width using these control parameters might enable us to perform easier simulation of a complex network such as a highway network with 3D terrain. Further investigation is in progress, both theoretically and experimentally, and will be reported in future.

Acknowledgments

Part of this work was financially supported by Japan Society for the Promotion of Science (Grant-in-Aid for Scientific Research No.26540129).

References

[1] J. D. Murray, "*Mathematical Biology I: An Introduction - Third Edition*," Chapter 13, Springer Science+Business Media, New York, 2001.
[2] O. Steinbock, Á. Tóth, K. Showalter, "Navigating Complex Labyrinths: Optimal Paths from Chemical Waves", *Science*, Vol.267, p.868, 1995.
[3] I. Lagzi, S. Soh, P. J. Wesson, K. P. Browne, B. A. Grzybowski, "Maze Solving by Chemotactic Droplets", *J. Am. Chem. Soc.*, Vol.132, p.1198, 2010.
[4] T. Nakagaki, H. Yamada, Á Tóth, "Maze-solving by an amoeboid organism", *Nature*, Vol.407, p.470, 2000.
[5] Y. Okabayashi, T. Isoshima, E. Nameda, S. Kim, M. Hara, "Two-Dimensional Nonlinear Fabry-Perot Interferometer: An Unconventional Computing Substrate for Maze Exploration and Logic Gate Operation.," *Int. J. Nanotech. Mol. Comp.*, Vol.3, p.13, 2011.
[6] T. Isoshima and Y. Ito, "Two-dimensional optical bistable device with external feedback for pulse propagation and spatio-temporal instability", *Proc.NOLTA2014*, p.625, 2014.
[7] T. Isoshima, "Control of wavefront propagation in two-dimensional bistable system", *Proc.NOLTA2017*, p.271, 2017.
[8] T. Isoshima, "Operation mode of wavefront propagation for maze exploration in two-dimensional optical bistable device", *Proc.NOLTA2018*, p.97, 2018.
[9] T. Isoshima, "Geometrical control of propagation properties in two-dimensional optical bistable devices", *Proc.NOLTA2019*, p.550, 2019.
[10] Université Pierre et Marie Curie and Laboratoire Jacques-Louis Lions, *FreeFEM++*, http://www.freefem.org/ff++/